Article

Not peer-reviewed version

UV Exposure Effects on Starch Films from *Solanum tuberosum* (Ecuadorian Potato): A Macro- and Nanoscale Investigation

Cynthia Pico , Pablo Ilvis , Santiago Casado *

Posted Date: 9 February 2026

doi: 10.20944/preprints202602.0589.v1

Keywords: starch films; potato starch; atomic force microscopy; UV irradiation; biopolymers

Preprints.org (www.preprints.org) | NOT PEER-REVIEWED | Posted: 9 February 2026 doi:10.20944/preprints202602.0589.v1

Article

UV Exposure Effects on Starch Films from *Solanum tuberosum* (Ecuadorian Potato): A Macro- and Nanoscale Investigation

Cynthia Pico [1], Pablo Ilvis [1] and Santiago Casado [1,2,*]

[1] Food and Biotechnology Science and Engineering Department, Universidad Técnica de Ambato, Ambato 180207, Ecuador
[2] Group for Universal Advance In bioScience (GUAIS), Universidad Técnica de Ambato, Ambato 180207, Ecuador
* Correspondence: s.casado@uta.edu.ec

Abstract

The growing pollution caused by plastics with slow degradation kinetics is demanding the search for biodegradable alternatives. Starch-based films are a promising option, but their practical application may be limited by their potential susceptibility to rapid ultraviolet (UV) exposure degradation. This study evaluates the effect of prolonged UV-C irradiation (254 nm, 168 h) on plasticizer-free films derived from the starch of the Ecuadorian potato *Solanum tuberosum* (*Chola* variety). Films formulated at 3 % and 5 % (w/v) starch were characterized before and after UV exposure. The analysis includes the evaluation of optical, mechanical, and physicochemical properties, along with Fourier Transform Infrared spectroscopy (FTIR) and atomic force microscopy (AFM) for nanoscale surface inspection. UV irradiation increased the opacity of the films but reduced slightly their tensile strength, elongation at break, moisture content, and total soluble matter. In contrast, the elastic modulus remained relatively high. FTIR analysis revealed no significant formation of new functional groups, suggesting that UV exposure induces a physical reorganization rather than chemical degradation. AFM measurements indicated that irradiation caused only minor nanoscale alterations in the same film regions. These alterations were more pronounced in films with higher starch concentrations. The results demonstrate that UV-C exposure induces minor structural adjustments in plasticizer-free starch films derived from the *Chola* variety, without compromising their fundamental integrity. Consequently, this work advances the understanding of the environmental stability of these films and supports their potential application as sustainable materials, even in conditions involving UV exposure.

Keywords: starch films; potato starch; atomic force microscopy; UV irradiation; biopolymers

1. Introduction

Environmental plastic pollution currently represents one of the most complex and persistent challenges [1–4]. Organic waste polymers can degrade in a few days at ambient conditions, whereas a common piece of petroleum-derived plastic may persist in the environment for up to five hundred years [5]. Several studies have shown that during degradation, these substances release micro-fragments that accumulate in numerous ecosystems and in animals across the planet [6–8]. It is estimated that approximately 25.3 million metric tons of plastic waste enter the oceans each year, of which about 16.8 million metric tons sink to the seabed, 6.6 million metric tons float as macroplastics, and 1.8 million metric tons accumulate on coastlines [9,10]. Micro- and nanoplastics have been identified not only as ubiquitous emerging pollutants but also as potential vectors for toxic substances

[11]. Their capability of crossing biological barriers and altering physiological processes has generated increasing scientific concern regarding their ecotoxicological implications [12–14].

These findings have intensified the search for sustainable, biodegradable alternatives that can reduce environmental impact while maintaining adequate performance. Biopolymers derived from renewable and abundant resources have been proposed as alternatives. Among these, starch has emerged as a promising substitute for conventional petroleum-based plastics due to its biodegradability and wide availability [15,16]. Their potential applications span the packaging, biomedicine, and agriculture sectors due to their transparency, barrier properties, and compatibility with biodegradable processing methods [17,18]. However, their behavior under ambient conditions and the limited mechanical strength of some biodegradable films may restrict their wider industrial application [18,19].

The mechanical and physicochemical properties of starch-based films are strongly influenced by their molecular structure, the preparation method, and the botanical source, with significant variations even among different varieties of the same species [20–23]. Ecuadorian potato starch (*Solanum tuberosum*) extracted from the *Chola* variety has been shown to produce films with greater strength and rigidity than those generated from other starch sources [20,24,25]. However, the environmental stability of these films when exposed to abiotic stress factors, such as ultraviolet (UV) irradiation, remains poorly understood, particularly in systems without plasticizers. Previous studies have reported that UV light can alter hydrogen bond networks, modify surface morphology, and affect the mechanical performance of polymeric films, depending on the material composition, UV exposure conditions, and wavelength [26,27].

This study evaluates the effect of prolonged exposure to UV-C light (254 nm) on films prepared from potato starch (*Solanum tuberosum, Chola* variety) at two different concentrations and without plasticizer. The films were characterized before and after UV irradiation using a combination of macro-, nano-, and chemical analysis techniques, including opacity assays, mechanical testing, Fourier-Transform Infrared (FTIR) spectroscopy, as well as solubility, moisture content, and Atomic Force Microscopy (AFM) measurements. Although clear differences were observed, the results demonstrate that irradiation leaves the core film structure largely intact, preserving its fundamental properties despite a slight reduction in efficacy.

2. Materials and Methods

2.1. Starch Extraction

Potato starch was extracted from the Ecuadorian potato (*Solanum tuberosum*), *Chola* variety. The extraction procedure followed the method proposed by Pico *et al*. [24]. The potatoes were washed and cut into small pieces and subsequently ground. Distilled water (1000 mL) was added to the resulting slurry, which was then filtered through gauze with an approximate pore size of 120 mesh. The filtrate was allowed to stand for 6 h to facilitate starch sedimentation. Subsequently, the supernatant was discarded, and the precipitate was dried in an oven at 45 ± 5 °C for approximately 12 h. The starch yield, expressed as a weight percentage relative to the fresh potato mass, was 13 %.

2.2. Film Preparation

Potato starch films were prepared by dispersing 3 and 5 g of starch in 100 mL of distilled water. Initially following the methodology described by Farhan and Hani [28], the suspensions were heated to 90 °C using a hot plate with magnetic stirring at a constant speed of 200 rpm. Subsequently, the samples were centrifuged at 7000 rpm and 25 °C for 15 min. The resulting supernatant was poured into 100 × 10 mm Petri dishes at a volume of 20 mL per dish. The plates were then dried in an incubator at 45 °C for 24 h and finally stored in a desiccator at room temperature.

2.3. Optical Characterization

The visual appearance and apparent transparency of each film sample were obtained using a conventional camera and diffused white light, placing the films onto a background containing black letters and figures.

Optical micrographs were taken by fixing square sections (approximately 10 mm per side) from each starch-based film under an EVOS XL microscope (Life Technologies, Thermo Fisher Scientific). Each sample was attached to a microscope slide using adhesive tape, positioned inverted, irradiated with transmitted white light, and inspected using a 40× magnification and 0.65 numerical aperture (in air) collimated objective.

2.4. Mechanical Properties

Tensile strength, elastic modulus, and elongation at the break of the films were determined under ambient conditions using a modified version of the ASTM D 882-88 standard method with a Brookfield CT3 texture analyzer (Ametek, Berwyn, PA, USA). Films were cut into rectangular strips measuring 50 mm in length and 20 mm in width. The separation speed between the crosshead was set at 0.5 mm/s, and the results were averaged from 7 replicates of each sample.

2.5. Fourier Transform Infrared Spectroscopy (FTIR)

Fourier transform infrared (FTIR) spectra were recorded as described by Orsuwan *et al.* [29], using a Spectrum Two spectrophotometer (Perkin-Elmer, Waltham, MA, USA) coupled to an attenuated total reflectance (ATR) adapter. All measurements covered a wave number range between 4000 and 500 cm^{-1} with 4 cm^{-1} accuracy. Under ambient conditions, samples of each film were located directly on the ATR tip surface and gently pressed with the flat-tip plunger. Data were acquired in triplicate at different locations of each film.

2.6. UV-Visible Optical Absorption and Opacity

To measure the opacity of the films, an accuSkan GO UV-Vis spectrophotometer (Thermo Fisher Scientific, Waltham, MA, USA) was employed. Samples were cut into rectangular pieces commensurate with the internal size of the quartz cells fitting the equipment. Measurements were performed in triplicate under ambient conditions, covering a wavelength range from 200 nm to 600 nm. Absorbance spectra were obtained by scanning the entire range and recording the reduction in intensity at each wavelength. Opacity (O) was calculated using Equation (1), where Abs_{560} represents the absorption at 560 nm wavelength.

$$O = \frac{Abs_{560}}{X} \tag{1}$$

Film thickness (X, mm) was measured using a 0.01 mm accuracy micrometer caliper, averaging the data from eight different locations on each film.

2.8. Moisture Content (MC)

For this test, a gravimetric method was applied using a conventional precision scale (0.01 mg accuracy). Samples of similar sizes were weighed without undergoing any prior treatment, and values were recorded as the initial weight (W_0). Subsequently, they were subjected to a drying process in an oven at 105 °C for 24 h. After the specified time, they were removed from the oven and placed into a desiccator with silica gel until they cooled down. Once acclimatized, they were weighed again, and values were recorded as the final weight (W_f). All measurements were performed in triplicate. The moisture content (MC) was calculated using Equation (2).

$$MC = \frac{W_0 - W_f}{W_0} * 100 \tag{2}$$

2.9. Water Total Soluble Matter (TSM)

Water solubility (Total Soluble Matter, *TSM*) was measured following the method described by Arancibia *et al.* [30] and Salazar *et al.* [31] using a conventional precision scale (0.01 mg accuracy). Square samples of approximately 5 mm sides from each film were weighed, and their initial weights (W_i) were obtained. Samples were then submerged into bottles containing 30 mL of distilled water. The bottles thus prepared were placed on a shaker operating at 70 rpm for 24 h at room temperature.

After retrieving the samples, they were stored at 105 °C for 24 h. Subsequently, the final dry weight (W_f) of each sample was determined, and their content of *TSM* was calculated using Equation (3).

$$TSM = \frac{W_i - W_f}{W_i} * 100 \tag{3}$$

2.10. Atomic Force Microscopy (AFM) Characterization

To characterize the surface of each starch film at the nanoscale, the Park System XE7 Atomic Force Microscope (AFM, Santa Clara, CA, USA) was used, following the methodology described by Ilvis *et al*. [20]. A small sample from each starch film was cut and mounted onto the AFM magnetic sample holder using double-sided adhesive tape. The measurements were performed in *tapping* mode under ambient conditions using NCHR cantilevers (nominal spring constant of 42 N/m, resonance frequency of 320 kHz, and tip diameter <10 nm). This dynamic mode has proven the capacity to measure both microscopic structures covered with debris [32] and for very soft samples [33]. The scan resolution was set to 512 × 512 pixels. AFM images were processed using XEI software version 5.1.6 (Park Systems, Santa Clara, CA, USA), applying linear background subtraction.

2.11. UV Exposure

The processed films were conditioned at 23 ± 2 °C and a relative humidity of 50 ± 5 % for 48 h. The films were then placed at a distance of 20 ± 2 cm from the irradiation source and irradiated using a UVP Sterilaire XX-20S lamp (UV-C, 254 nm, 20 W) for 168 h of continuous exposure. Control samples were maintained under identical environmental conditions without UV exposure. After irradiation, the samples were reconditioned prior to mechanical, physicochemical, and surface characterization.

2.12. Statistical Analysis

The statistical analysis was conducted by determining variance (ANOVA) and Tukey's multiple comparison tests at a 95 % confidence level using the R 4.4.0 software (R Development Core Team, Vienna, Austria).

3. Results and Discussion

3.1. Optical Characterization of the Films

The apparent transparency of the films prepared from starch extracted from the *Chola* potato variety is shown in Figure 1. Control starch films showed significantly higher transparency than the UV-irradiated films. The higher transparency of the control films is typical of potato starch-based materials, possibly due to factors that favor greater light transmittance and optical clarity, such as the morphology of the starch granules, high swelling capacity, and phosphate monoester content [34]. In contrast, when the films were exposed to UV irradiation, they became visibly more opaque, with a yellowish color.

This increase in the apparent opacity may be related to structural changes occurring on the surface of the films, associated with chemical processes such as a different entanglement of molecules during exposure. UV light could induce bond breakage and generate free radicals in the outer layer of the films, which may subsequently recombine to form covalent bonds, reducing molecular mobility and resulting in a more rigid and compact polymeric structure, as has been described for some polymeric films exposed to UV radiation [35–37].

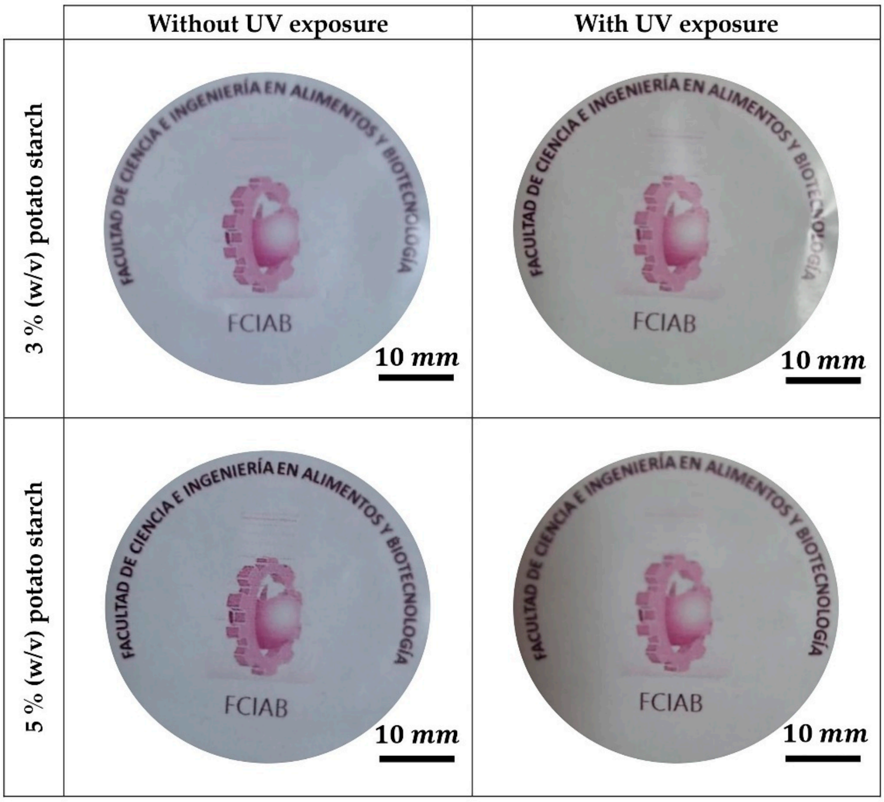

Figure 1. Apparent transparency of *Chola* potato starch films with and without UV exposure.

Optical microscopy using white transmitting light revealed differences between the structures of each sample, as shown in Figure 2. Films not irradiated with UV light showed a more transparent appearance, with lower apparent opacity and higher intensity contrast, compared to the films exposed to UV radiation. These observations are consistent with previous reports on starch-based films, where increased matrix density and structural rearrangements decrease light transmission and optical contrast following external treatments [38].

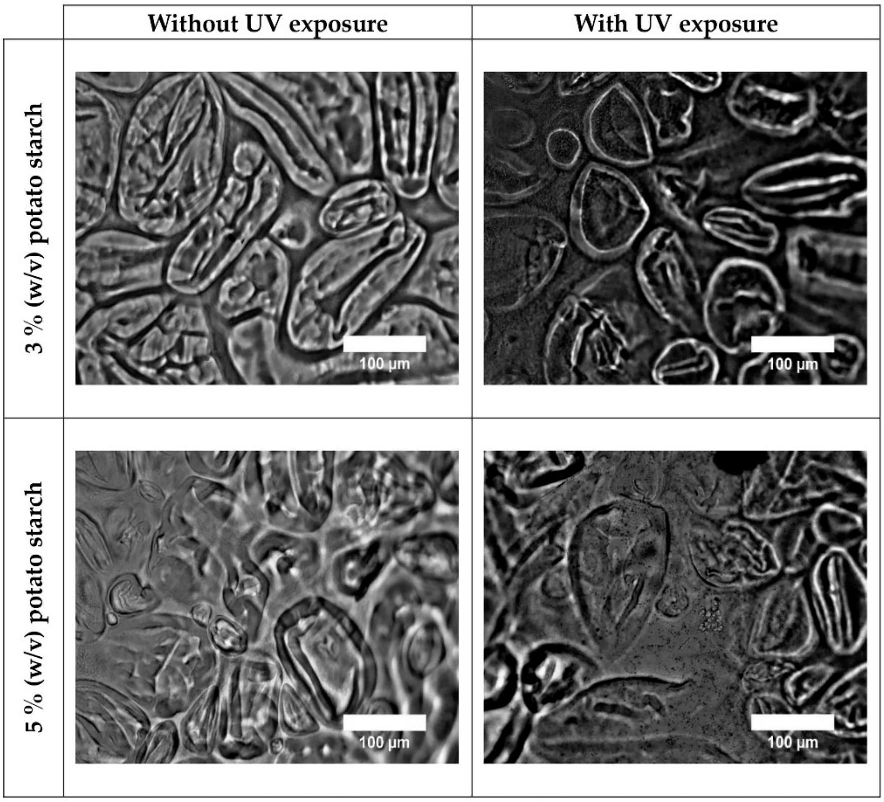

Figure 2. White light transmission optical microscopic images of *Chola* potato starch film samples with and without UV exposure.

3.2. Mechanical Properties

Figure 3 compares the tensile strength, modulus of elasticity, and elongation at break of the films with varying *Chola* potato starch content, both before and after exposure to UV radiation.

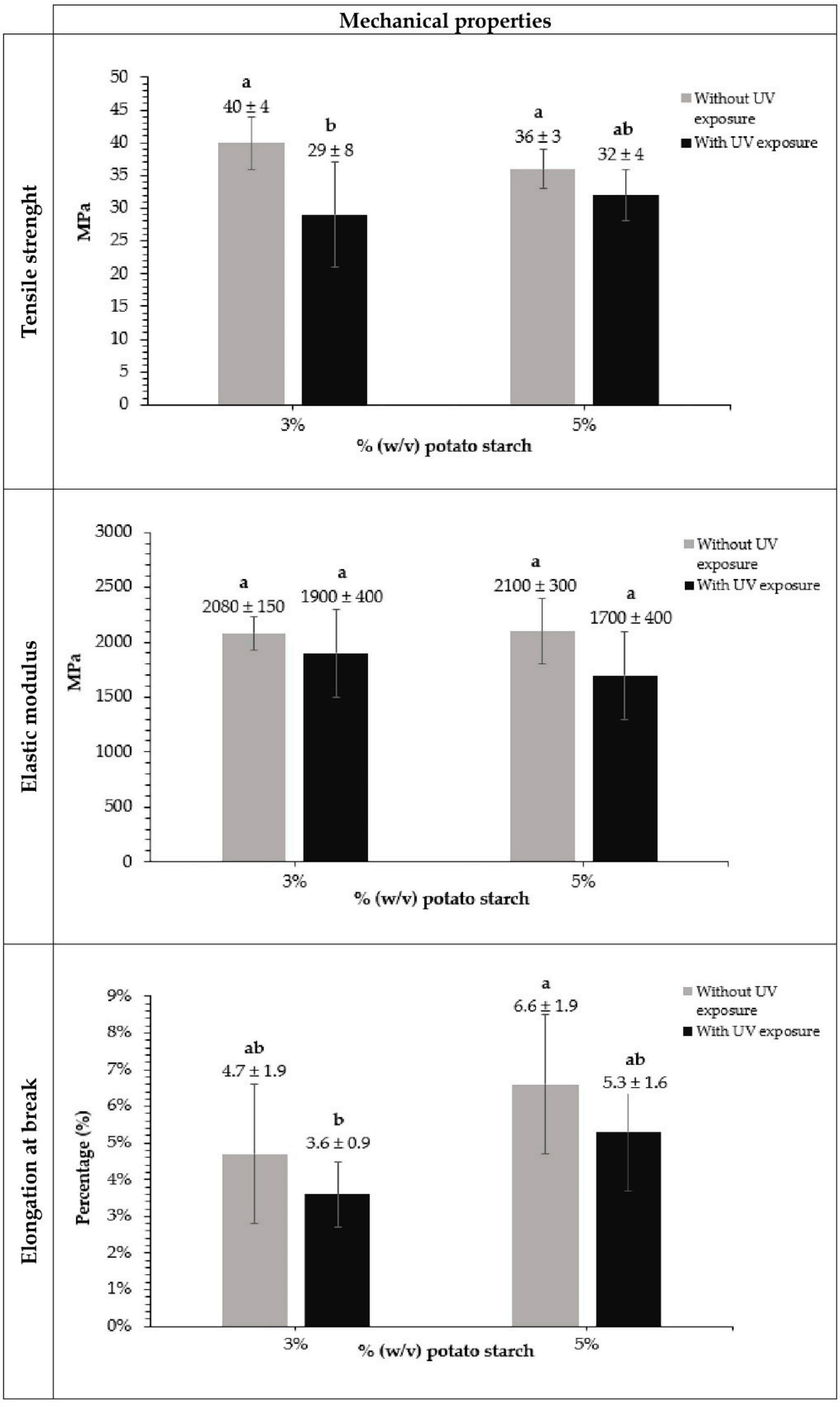

Figure 3. Mechanical properties of potato starch films with and without UV exposure, at different starch concentrations. The data shown are representative of seven independent experiments and comprise each mean ± SD. Different letters (a, b) indicate significant differences between the different films ($p \leq 0.05$).

Films not exposed to UV radiation exhibited higher tensile strength (40 ± 4 MPa and 36 ± 3 MPa for 3 % and 5 % (w/v) potato starch, respectively). After UV exposure, these values decreased to 29 ± 8 MPa and 32 ± 4 MPa for 3 % and 5 % (w/v) potato starch, respectively. The values without exposure were similar to those reported by Ilvis *et al*. [20] and higher than those reported by Dutta and Sig [39]. Films with higher starch concentrations showed a smaller difference, which could be related to the fact that starch forms a polymer network with greater density and stability [40]. Ilvis *et al*. [20] mention that the *Chola* variety potato has a high amylose content, which could contribute to greater strength in the polymer network. Furthermore, during the film manufacturing process, the starch solution was centrifuged after gelatinization to enrich the supernatant with a higher amount of amylose.

The elastic modulus obtained before exposure of the films was 2080 ± 150 MPa and 2100 ± 300 MPa for the films with 3 % and 5 % (w/v) potato starch, respectively, indicating that the films exhibit high initial stiffness. These values are similar to those reported by Ilvis *et al*. [20] for *Chola* potato starch and higher than those reported by Pico *et al*. [24] and Domene Lopez *et al*. [41] for starch extracted from different potato varieties. The 3 % (w/v) starch films exposed to UV irradiation showed slight changes in the elastic modulus (from 2080 ± 150 MPa to 1900 ± 400 MPa), while the 5 % (w/v) starch films showed a moderate decrease from 2100 ± 300 MPa to 1700 ± 400 MPa. At both concentrations, a high value was maintained after UV light exposure, suggesting that the polymer network retains its overall structural stability.

The elongation at break for 3 % and 5 % (w/v) starch content films before exposure was 4.7 ± 1.9 % and 6.6 ± 1.9 %, respectively. These values are similar to those revealed by Ilvis *et al*. [20], for the potato variety *Chola* without glycerol, where elongations close to 6 % were reported, attributed to the amount of amylose and a compact polymeric network. In contrast, studies by Dai, Zhang, and Cheng [42] show elongations in a range of 46 % to 51.66 %, although in this case glycerol was added. In this particular research, more ductile and less rigid films were obtained, possibly due to the addition of the plasticizing agent, which reduces the rigid intermolecular interactions and increases the mobility in the polymeric chains. After exposure to UV irradiation, the elongation at break shows a minor descent, resulting in a slightly more brittle film.

3.3. Fourier Transform Infrared Spectroscopy (FTIR) Absorption

Fourier transform infrared spectroscopy (FTIR) permits the observation of characteristic bands corresponding to specific chemical bonds present in each film. The spectrograms obtained with and without exposure are shown in Figure 4.

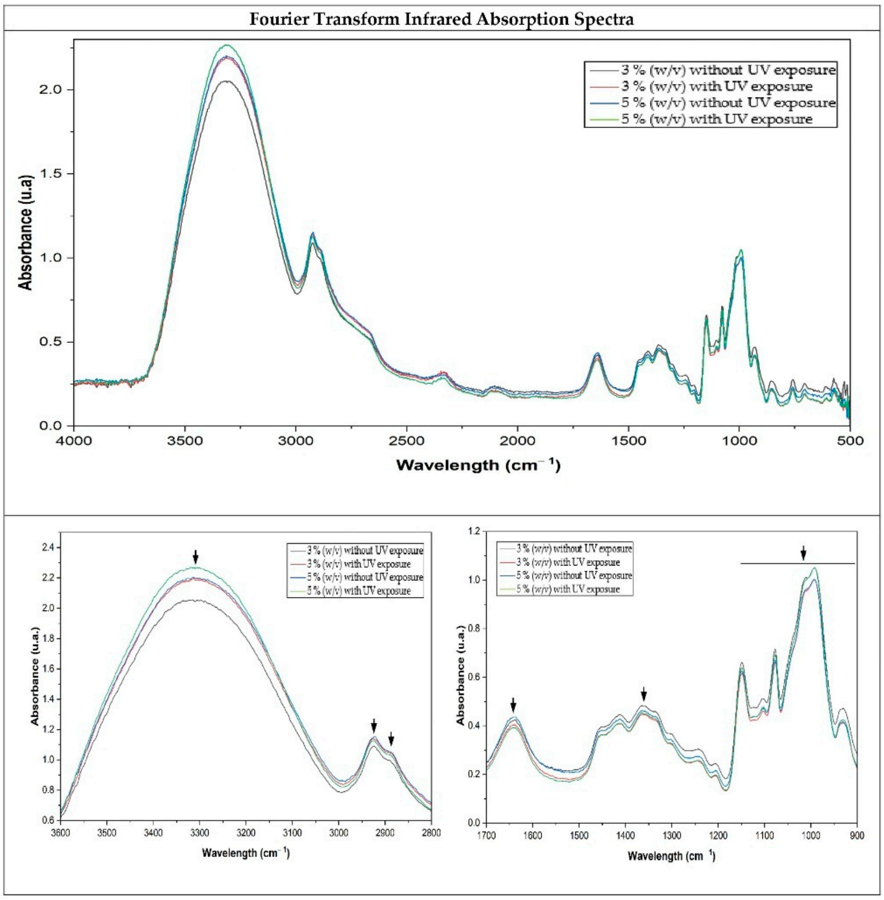

Figure 4. Infrared absorption spectra by Fourier transform obtained in each of the films produced. Arrows highlight representative peaks.

The spectra obtained at different starch concentrations without UV exposure are similar to the characteristic bands obtained previously [20,24]. The region between 3600 cm⁻¹ and 3200 cm⁻¹ is attributed to the stretching of the hydroxyl (OH) groups present in the starch chains and absorbed water. This region shows sensitivity to moisture content, indicating the existence of a hydrogen bond network that maintains the film structure [20]. The region between 2940 cm⁻¹ and 2840 cm⁻¹ is attributed to C-H stretching vibrations, corresponding to the main chains of the starch polymer [43]. Furthermore, the band around 1638 cm⁻¹ represents bending vibrations of the absorbed water, while the bands between 1390 cm⁻¹ and 1380 cm⁻¹ are related to bending vibrations of the COH group [44]. The bands between 1200 cm⁻¹ and 900 cm⁻¹ correspond to the stretching vibrations of C-O, C-C and COH, in the starch structure [45].

An increase in intensity after UV light exposure was observed in the band between 3200 cm⁻¹ and 3400 cm⁻¹, corresponding to the stretching of the (-OH) group [46]. This could indicate water loss and a possible reorganization of the hydrogen network due to physical modifications in the polymer matrix. Meanwhile, in the region between 1200 cm⁻¹ and 900 cm⁻¹, corresponding to the C-O, C-C, and COH vibrations, a slight change in the bands was observed; this change was more noticeable in the films made with 5 % (w/v) starch. This could be related to a higher density of intermolecular bonds in the matrix, which facilitates the reorganization of the structures upon interaction with UV radiation [47].

Bajer, Kaczmarek, and Bajer [48] and Gutiérrez-Silva [49] reported that UV irradiation of films from different sources and in the absence of plasticizers leads to modifications in the intensity of the hydroxyl bands in the 3200–3400 cm⁻¹ region and alterations in the fingerprint region. Similarly, Shahabi, Goudarzi, and Babaei [50] reported that starch films containing plasticizers exhibit spectral changes associated with hydrogen bond reorganization and water loss, without evidence of oxidative phenomena. Therefore, these results suggest that starch films prepared at different concentrations and in the absence of plasticizers, when subjected to UV irradiation underwent a physical reorganization of the polymer network without inducing appreciable chemical degradation.

3.4. Optical Absorption

Figure 5 shows the spectra obtained at 200–600 nm from starch films at different starch percentages with and without UV exposure.

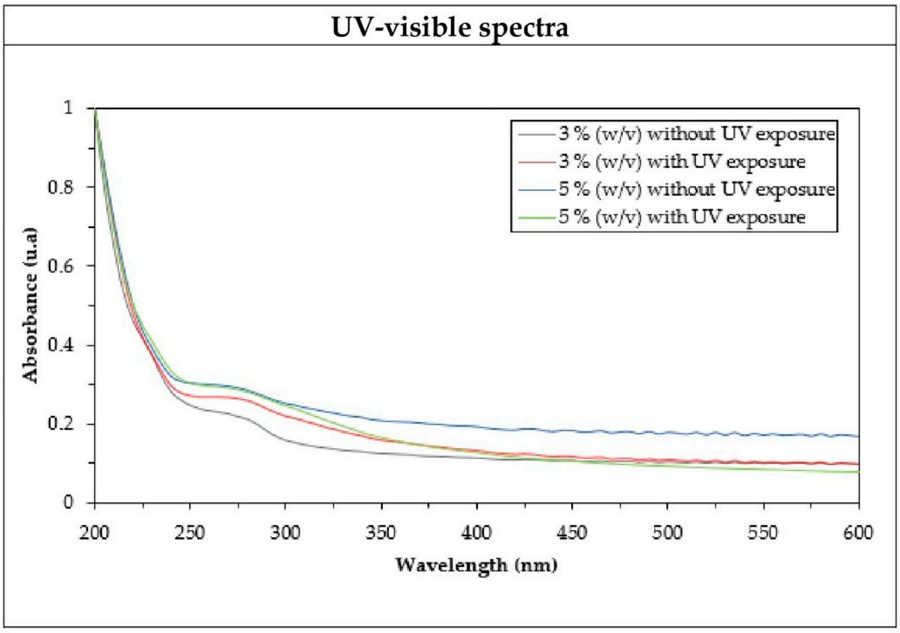

Figure 5. UV-Vis spectra of starch films prepared from 3 % and 5 % (w/v) solutions, before and after UV irradiation.

The UV-Vis spectrophotometric analysis of potato starch films reveals high absorbance values in the UV region (200–250 nm) and a progressive decrease towards the visible region (300–600 nm).

When comparing samples exposed and not exposed to UV irradiation, an increase in absorbance was observed in the irradiated films, particularly in the UV and near-UV regions. This suggests the possible formation of species with greater absorption or reflection capacity in this region of the spectrum, which could be related to photo-induced processes in the polymer matrix, such as oxidation phenomena or a rearrangement of the existing functional groups.

Thickness of all the films explored in this analysis is shown in Table 1.

Table 1. Thickness (µm) of each film with different percentages of potato starch with and without exposure to UV irradiation.

% (w/v) potato starch	*Treatment*	Thickness (µm)
3	Without UV exposure	82 ± 23^{ab}
3	With UV exposure	71 ± 15^{b}
5	Without UV exposure	114 ± 14^{a}
5	With UV exposure	113 ± 12^{a}

Different letters (a, b) within the column indicate significant differences ($p \leq 0.05$) according to Tukey's test. Data shown correspond to the measurements performed with eight replicates and represent the mean ± SD.

Table 2 presents the opacity values obtained through the thickness indicated in Table 1 and the absorbances measured at 560 nm.

Table 2. The opacity measured on potato starch films with and without UV irradiation.

% (w/v) potato starch	*Treatment*	Opacity (AU/mm)
3	Without UV exposure	1.00 ± 0.02^{b}
3	With UV exposure	2.12 ± 0.02^{a}
5	Without UV exposure	0.83 ± 0.02^{b}
5	With UV exposure	2.41 ± 0.02^{a}

Different letters (a, b) within the column indicate significant differences ($p \leq 0.05$) according to Tukey's test. Data shown correspond to the measurements performed with three replicates and represent the mean ± SD.

At both starch concentrations of 3 % and 5 % (w/v) the opacity values before UV irradiation are low and show no significant differences between them (1.00 mm^{-1} and 0.83 mm^{-1}, respectively), indicating high transparency at this wavelength. This behavior could be related to a relatively homogeneous polymer structure that allows for efficient light transmission through the films. Previous studies on starch-based edible films have demonstrated that starch concentration plays a key role in determining optical properties by influencing matrix homogeneity and light scattering behavior [20,51]. After the films are exposed to UV light, a significant increase in opacity is observed in the two starch concentrations analyzed.

This effect may be attributed to UV-induced cleavage of glycosidic bonds and partial oxidation of starch chains, leading to the formation of free radicals, which act as centers for light absorption or scattering, thereby reducing optical transmittance [37]. In addition, UV irradiation may promote molecular rearrangements and local variations in film density, generating internal heterogeneities that enhance light reflection and scattering within the films.

3.5. Moisture Content (MC)

Moisture content results are shown in Table 3.

Table 3. Moisture content (MC) of potato starch films with and without UV irradiation.

% (w/v) potato starch	*Treatment*	Moisture content (%)
3	Without UV exposure	11.5 ± 0.5^{a}
3	With UV exposure	7.1 ± 0.8^{b}
5	Without UV exposure	11.6 ± 0.6^{a}
5	With UV exposure	6.8 ± 0.6^{b}

Different letters (a, b) in the same column indicate significant differences between the different films ($p \leq 0.05$). Data shown correspond to the measurements performed with three replicates and represent the mean ± SD.

The moisture content at concentrations of 3 % and 5 % (w/v), without exposure to UV irradiation, showed low values (11.5 % and 11.6 %, respectively). This indicates that the films exhibit high cohesion of the polymer matrix and a lower water retention capacity, possible due to structural compaction and reduced mobility of the starch chains. The values obtained are similar to those reported previously [20,52].

When the films were exposed to UV light, the moisture content decreased significantly to 7.1 % for films with 3 % (w/v) starch concentration and to 6.8 % for films with 5 % (w/v). This could be attributed to photo-dehydration processes and possible hydrogen bond network reorganization processes that reduce the films' water absorption capacity. Previous studies have reported that in thermoplastic starch films, UV causes oxidation and chain cleavage, reducing the hydroxyl sites available to form hydrogen bonds with water [35,53]. The study published by Uyarcan and Güngör [54] also reports that UV light decreases surface moisture and hygroscopic capacity of starch-based films, by losing bound water and undergoing slight structural shrinkage, which results in drier films that are more stable against ambient moisture absorption.

3.6. Water Total Soluble Matter (TSM)

Table 4 shows the total soluble matter content in water measured on the samples.

Table 4. Total Soluble Matter (TSM) in water for films prepared with two starch concentrations, measured with and without UV irradiation of the films.

% (w/v) potato starch	***Treatment***	**TSM (%)**
3	Without UV exposure	28.1 ± 0. 6^a
3	With UV exposure	17.7 ± 0.8^b
5	Without UV exposure	29.2 ± 0.6^a
5	With UV exposure	18.6 ± 1.0^b

Different letters (a, b) in the same column indicate significant differences between the different films ($p \leq 0.05$). Data shown correspond to the measurements performed with three replicates and represent the mean ± SD.

TSM of films without UV exposure did not vary significantly with starch percentage and exhibited high values, similar to those obtained previously [20]. A high TSM value indicates low crystallinity, probably influenced by the amylose/amylopectin ratio of the starch. After UV exposure, TSM decreases at both starch concentrations, indicating that the films exhibit greater internal cohesion and lower solubility. According to Quispe, López, and Villar [35] and Uyarcan and Güngör [55], UV exposure induces a mild oxidation and crosslinking process, resulting in a denser and less soluble structure. The observed decrease in TSM suggests the formation of a polymer network with greater stability against hydrolytic degradation processes, confirming the MC analysis.

3.8. Nanoscopic Characterization

Figure 6 shows Atomic Force Microscopy (AFM) images acquired in *tapping* mode, presenting a comparison of the surface topographies in the same areas of the potato starch films with starch concentrations of 3 % and 5 % (w/v), both with and without UV exposure, at two different scan sizes. All films without UV exposure showed a predominantly granular morphology, probably associated with the presence of domains derived from partially gelatinized starch granules used in their preparation, which generates a micro-rough surface characteristic of polysaccharide-based matrices after drying [41,55]. Surface topography became more heterogeneous in the 5 % (w/v) samples, with more pronounced elevations and depressions, probably caused by a higher density of amylose and amylopectin chains, which promotes intermolecular aggregation during the drying process. Nevertheless, despite this granular structure, surfaces appear quite united at this scale in all the cases analyzed.

doi:10.20944/preprints202602.0589.v1

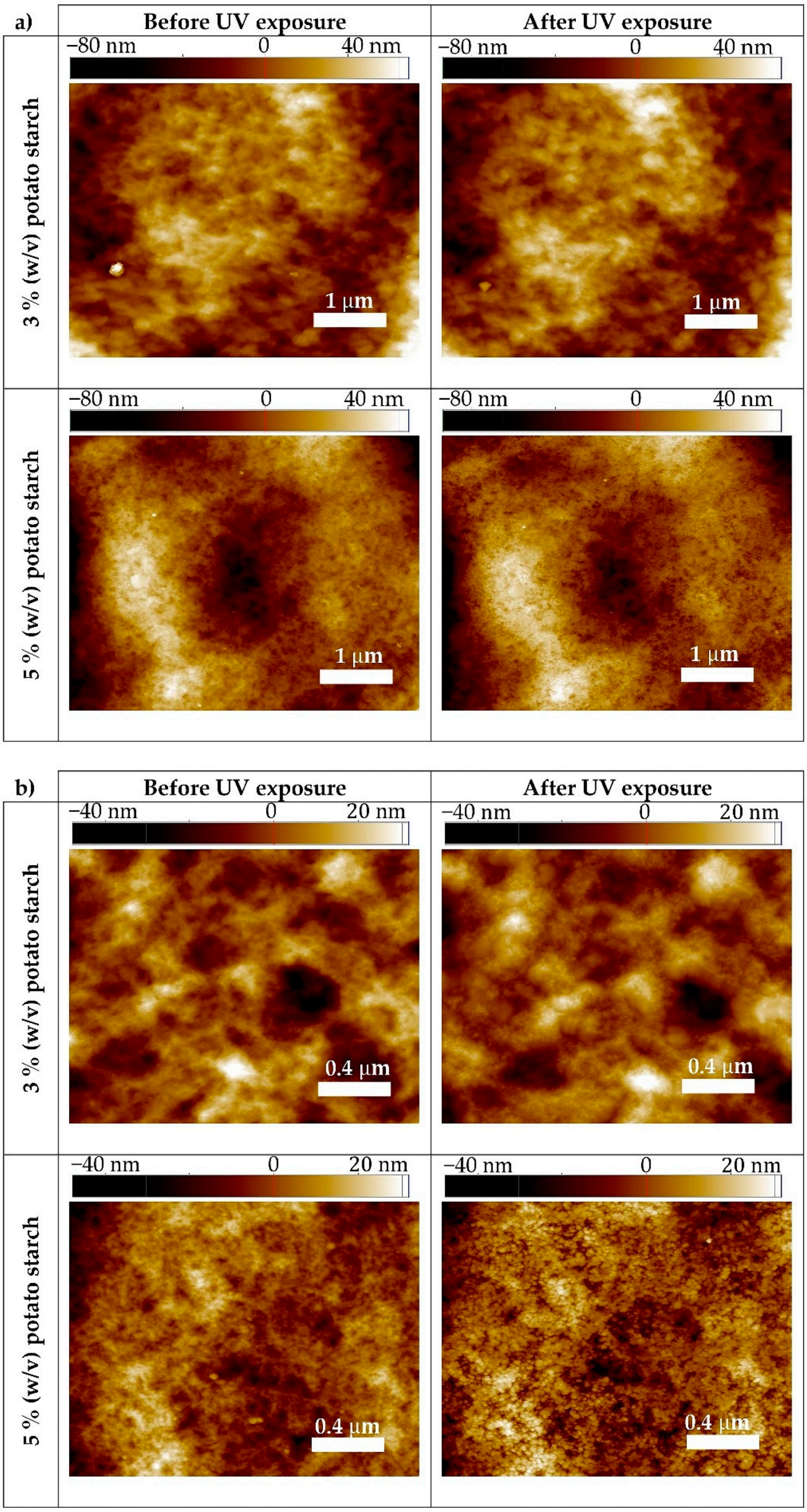

Figure 6. Atomic Force Microscopy (AFM) topographic images in *tapping* mode obtained on the surface of films from each potato starch concentration, before and after exposure to UV irradiation in the same regions at scan sizes of 5 x 5 µm² (a) and 2 x 2 µm² (b).

After UV exposure, exactly the same regions were found and measured again, which allows the comparison of the topography of the surface at the nanoscale. This permits detecting modifications caused only by the UV-C light and not by the intrinsic roughness heterogeneity of the samples. Slight changes in the surface topography are observed at both concentrations and span ranges, although the main structure was maintained in all cases. Clearer differences are detected on the films prepared with 5 % (w/v) starch concentration at the smallest scan size analyzed, showing more separated protrusions. This suggests that higher starch concentrations may promote UV energy absorption and amplify structural changes within the polymer matrix, perhaps due to a local structural reorganization and partial crosslinking processes when subjected to UV radiation.

To further corroborate the minor differences found between AFM topographic images before and after irradiation, a roughness comparison is performed. Choosing the Root Mean Square (RMS, Rq) parameter, a small increase in roughness is observed in all the cases analyzed (Table 5), confirming the previous observation. This suggests that the topographic modifications induced by UV irradiation only promote low magnitude topographic adjustments, without causing significant structural alterations on the surface.

Table 5. Root Mean Square (RMS, Rq) (nm) roughness values of the 2 x 2 μm² and 5 x 5 μm² topographic images obtained by AFM from each of the films at different percentages of potato starch before and after exposure to UV irradiation.

% (w/v) potato starch	2 x 2 μm²		5 x 5 μm²	
	Before UV exposure	After UV exposure	Before UV exposure	After UV exposure
3	13 ± 6^a	13 ± 7^a	29 ± 9^a	31 ± 11^a
5	9 ± 5^a	10 ± 6^a	23 ± 8^a	26 ± 10^a

Similar letters (a) in the row indicate no significant differences between the different films ($p > 0.05$). Data shown correspond to the measurements performed in three areas and represent the mean ± SD.

4. Conclusions

Starch-based films without plasticizers, derived from Ecuadorian *S. tuberosum* (*Chola* variety) at two different concentrations, were analyzed both before and after prolonged UV-C irradiation (wavelength: 254 nm). The study systematically evaluated their physicochemical, mechanical, and nano-structural properties. The findings revealed that UV exposure induces several minor modifications in these films, although the core structure preserves its fundamental integrity.

At the macroscopic level, irradiation led to a marked increase in film opacity and the development of a yellowish coloration, indicating reduced light transmittance that may be associated with structural rearrangements within the polymeric matrix. However, although the treated films exhibited a minor decrease in tensile strength and elongation at break, their elastic modulus remained relatively high, suggesting that the starch network preserves its overall structure, despite becoming slightly more brittle.

FTIR spectroscopy confirmed that UV light does not generate significant new functional groups, indicating that the observed changes are predominantly physical rather than chemical. The observed reduction in moisture content and total soluble matter indicates a decrease in hydrophilic interactions, which could be attributed to factors such as an internal densification of the polymer network. This suggests an enhanced resistance to water uptake and dissolution after UV irradiation.

At the nanoscale, the same surface topography was inspected on each sample before and after UV exposure using AFM. Moderate changes were detected, which were clearer for the most concentrated sample. However, although an increase in surface heterogeneity and roughness was observed, the primary structure remained largely intact even at this scale.

In conclusion, these promising plasticizer-free starch-based films, derived from Ecuadorian *S. tuberosum* (*Chola* variety), have proved exceptional performance not only at ambient conditions but also under UV-C irradiation. These findings provide valuable insights into the search for ecological films and highlight their potential for use in sustainable applications where exposure to ultraviolet radiation is unavoidable.

Author Contributions: Conceptualization, C.P. and S.C.; methodology, C.P., P.I., and S.C.; software, C.P., P.I., and S.C.; validation, C.P., P.I., and S.C.; formal analysis, C.P., P.I., and S.C.; investigation, C.P., P.I., and S.C.; resources, C.P. and S.C.; data curation, C.P., P.I., and S.C.; writing—original draft preparation, C.P., P.I., and

S.C.; writing—review and editing, C.P., P.I., and S.C.; visualization, C.P., P.I., and S.C.; supervision, S.C. All authors have read and agreed to the published version of the manuscript.

Funding: This research received no external funding.

Data Availability Statement: Not applicable, since data obtained are presented directly in the article.

Acknowledgments: Authors greatly acknowledge Universidad Técnica de Ambato (UTA) and its "*Dirección de Investigación y Desarrollo (DIDE)*" Department for their support and equipment acquisition. S.C. thanks the "*Canje de Deuda Ecuador-España – Extensión*" program for the AFM procurement. P.I. thanks to V.E. and M.C. for their support.

Conflicts of Interest: The authors declare no conflict of interest.

References

1. Borrelle, S.B.; Ringma, J.; Law, K.L.; Monnahan, C.C.; Lebreton, L.; McGivern, A.; Murphy, E.; Jambeck, J.; Leonard, G.H.; Hilleary, M.A.; et al. Predicted Growth in Plastic Waste Exceeds Efforts to Mitigate Plastic Pollution. *Science* **2020**, 369, 1515–1518. https://doi.org/10.1126/science.aba3656
2. Fayshal, M.A. Current Practices of Plastic Waste Management, Environmental Impacts, and Potential Alternatives for Reducing Pollution and Improving Management. *Heliyon* **2024**, 10, e40838. https://doi.org/10.1016/j.heliyon.2024.e40838
3. Rana, R.; Mishra, A.; Goswami, R.; Ahmad, A.; Ahmad, W. Plastics and the Environment: Challenges, Impacts, and Pathways to Sustainability. *Integr. Environ. Assess. Manage.* **2025**, vjaf193. https://doi.org/10.1093/inteam/vjaf193
4. Kibria, Md.G.; Masuk, N.I.; Safayet, R.; Nguyen, H.Q.; Mourshed, M. Plastic Waste: Challenges and Opportunities to Mitigate Pollution and Effective Management. *Int. J. Environ. Res. Public Health* **2023**, 17, 20. https://doi.org/10.1007/s41742-023-00507-z
5. Shashoua, Y.; Peydaei, A.; Mortensen, M.N.; Kanstrup, A.B.; Gregory, D.J. Physio-Chemical Degradation of Single-Use Plastics in Natural Weather and Marine Environments. *Environ. Pollut.* **2024**, 357, 124414. https://doi.org/10.1016/j.envpol.2024.124414
6. Yousafzai, S.; Farid, M.; Zubair, M.; Naeem, N.; Zafar, W.; Zaman Asam, Z.U.; Farid, S.; Ali, S. Detection and Degradation of Microplastics in the Environment: A Review. *Environ. Sci.: Adv.* **2025**, 4, 1142–1165. https://doi.org/10.1039/D5VA00064E
7. Dziobak, M.K.; Fahlman, A.; Wells, R.S.; Takeshita, R.; Smith, C.; Gray, A.; Weinstein, J.; Leslie B.H. First evidence of microplastic inhalation among freeranging small cetaceans. *PLoS ONE* **2024**, 19, 10, e0309377. https://doi.org/10.1371/journal.pone.0309377
8. Pradel, A.; Hufenus, R.; Schneebeli, M.; Mitrano, D.M. Impact of contaminant size and density on their incorporation into sea ice. *Nat. Commun.* **2025**, 16, 4375. https://doi.org/10.1038/s41467-025-59608-2
9. Isobe, N.; Ishii, S.; Nomaki, H. Progress and prospects in polymer science addressing plastic pollution in marine environments, including the deep-sea floor. *Curr. Opin. Chem. Eng.* **2025**, 47, 101089. https://doi.org/10.1016/j.coche.2024.101089
10. Yin Feng, T.; Nur Hidayah, M.I.; Han Lyn, F.; Nur Hanani, Z.A. Physical and Functional Properties of Pulsed-Ultraviolet Treated Starch Based Films with Papaya Leaf Extract. *Sustainable Food Technol.* **2025**, 3, 1986–1995, https://doi.org/10.1039/D5FB00350D
11. Oliveira, M.; Almeida, M. The why and how of micro(nano)plastic research. *TrAC Trends Anal. Chem.* **2019**, 114, 196–201. https://doi.org/10.1016/j.trac.2019.02.023
12. Yousefi, M.; Mazaheri, Y.; Soltani, M.; Rezagholizade-shirvan, A.; Sadighara, P.; Askari, E.; Salehi, A.; Alikord, M.; Shokri, S. Microplastics as emerging contaminants in the food chain: Assessing exposure and threats to consumers, *Food Biosci.* **2025**, 74, 108035. https://doi.org/10.1016/j.fbio.2025.108035
13. Hu, C.J.; Garcia, M.A.; Nihart, A.; Liu, R.; Yin, L.; Adolphi, N.; Gallego, D.F.; Kang, H.; Campen, M.J.; Yu, X. Microplastic presence in dog and human testis and its potential association with sperm count and weights of testis and epididymis, *Toxicol. Sci.* **2024**, 200, 2, 235–240. https://doi.org/10.1093/toxsci/kfae060
14. Tavakolpournegari, A.; Villacorta, A.; Morataya-Reyes, M.; Arribas Arranz, J.; Banaei, G.; Pastor, S.; Velázquez, A.; Marcos, R.; Hernández, A.; Annangi, B. Harmful effects of true-to-life nanoplastics derived

from PET water bottles in human alveolar macrophages. *Environ. Pollut.* **2024**. 348, 123823. https://doi.org/10.1016/j.envpol.2024.123823

15. Kossalbayev, B.D.; Belkozhayev, A.M.; Abaildayev, A.; Kadirshe, D.K.; Tastambek, K.T.; Kurmanbek, A.; Toleutay, G. Biodegradable Packaging from Agricultural Wastes: A Comprehensive Review of Processing Techniques, Material Properties, and Future Prospects. *Polymers* **2025**, 17, 2224. https://doi.org/10.3390/polym17162224
16. Balart, R.; Garcia-Garcia, D.; Fombuena, V.; Quiles-Carrillo, L.; Arrieta, M.P. Biopolymers from Natural Resources. *Polymers* **2021**, 13, 2532. https://doi.org/10.3390/polym13152532
17. Arruda, T.R.; Machado, G.d.O.; Marques, C.S.; Souza, A.L.d.; Pelissari, F.M.; Oliveira, T.V.d.; Silva, R.R.A. An Overview of Starch-Based Materials for Sustainable Food Packaging: Recent Advances, Limitations, and Perspectives. *Macromol* **2025**, *5*, 19. https://doi.org/10.3390/macromol5020019
18. Lescano, M.; Vásquez, N.; Tarrillo, S.; Yoplac, I.; Velásquez-Barreto, F.F. Development and Optimization of Biofilms Made from Potato or Arracacha. *Starch-Stärke* **2021**, 73, 2100075. https://doi.org/10.1002/star.202100075
19. Magnaghi, L.S.; Trigueros, E.; Biesuz, R. A Statistical Approach toward Biofilms Hydrophilicity Characterization: Integrating ANOVA, DOE, and PCA for Starch/Glycerol/CMC Films Case Study. *ACS Appl. Bio Mater.* **2025**, 8, 5, 3691–3696. https://doi.org/10.1021/acsabm.5c00510
20. Ilvis, P.; Acosta, J.; Arancibia, M.; Casado, S. Nanoscopic Characterization of Starch-Based Biofilms Extracted from Ecuadorian Potato (*Solanum tuberosum*) Varieties. *Polymers* **2024**, *16*, 1873. https://doi.org/10.3390/polym16131873
21. Aurora-Vigo, E.F.; Paucar-Menacho, L.M.; Anaya-Esparza, L.M.; Schmiele, M. Oca (Oxalis tuberosa Mol.): An Andean Tuber With Promising Physicochemical, Technological and Nutritional Properties for Potential Industrial Applications. *Plant Foods for Hum. Nutr.* **2025**, 80, 179. https://doi.org/10.1007/s11130-025-01427-3
22. Vera, W.; Quevedo-Olaya, J.L.; Minchán-Velayarce, H.; Samaniego-Rafaele, C.; Rodríguez-León, A.; Salvador-Reyes, R.; Quispe-Santivañez, G.W. From Ethnobotany to Food Innovation: Applications and Functional Potential of *Mashua (Tropaeolum tuberosum)*. *Foods* **2025**, *14*, 4091. https://doi.org/10.3390/foods14234091
23. Luera-Quiñones, S.; Correa, M.J.; Moreno-Rojo, C.; Salvador-Reyes, R.; Paucar-Menacho, L.M. *Mashua* (*Tropaeolum tuberosum* Ruiz & Pavón): Nutritional Composition, Bioactive Compounds, and Functional Potential as an Andean Natural Ingredient. *Foods* **2025**, *14*, 4198. https://doi.org/10.3390/foods14244198
24. Pico, C.; De La Vega, J.; Tubón, I.; Arancibia, M.; Casado, S. Nanoscopic Characterization of Starch Biofilms Extracted from the Andean Tubers *Ullucus Tuberosus*, *Tropaeolum Tuberosum*, *Oxalis Tuberosa*, and *Solanum Tuberosum*. *Polymers* **2022**, 14, 4116. https://doi.org/10.3390/polym14194116
25. Karnwal, A.; Rauf, A.; Jassim, A.Y.; Selvaraj, M.; Al-Tawaha, A.R.M.S.; Kashyap, P.; Kumar, D.; Malik, T. Advanced Starch-Based Films for Food Packaging: Innovations in Sustainability and Functional Properties. *Food Chem.: X* **2025**, 29, 102662. https://doi.org/10.1016/j.fochx.2025.102662
26. Zhou, J.; Zhang, J.; Ma, Y.; Tong, J. Surface Photo-Crosslinking of Corn Starch Sheets. *Carbohydr. Polym.* **2008**, 74, 405–410. https://doi.org/10.1016/j.carbpol.2008.03.006
27. Fathi, N.; Almasi, H.; Pirouzifard, M.K. Effect of Ultraviolet Radiation on Morphological and Physicochemical Properties of Sesame Protein Isolate Based Edible Films. *Food Hydrocoll.* **2018**, 85, 136–143. https://doi.org/10.1016/j.foodhyd.2018.07.018
28. Farhan, A.; Hani, N.M. Characterization of Edible Packaging Films Based on Semi-Refined Kappa-Carrageenan Plasticized with Glycerol and Sorbitol. *Food Hydrocoll.* **2017**, 64, 48–58. https://doi.org/10.1016/j.foodhyd.2016.10.034
29. Orsuwan, A.; Sothornvit, R. Development and Characterization of Banana Flour Film Incorporated with Montmorillonite and Banana Starch Nanoparticles. *Carbohydr. Polym.* **2017**, 174, 235–242. https://doi.org/10.1016/j.carbpol.2017.06.085

doi:10.20944/preprints202602.0589.v1

30. Arancibia, MY; Alemán, A.; López-Caballero, ME; Gómez-Guillén, MC; Montero, P. Development of active films of chitosan isolated by mild extraction with added protein concentrate from shrimp waste. *Food Hydrocoll*. **2015**, 43, 91–99. https://doi.org/10.1016/j.foodhyd.2014.05.006
31. Salazar, D.; Arancibia, M.; Casado, S.; Viteri, A.; López-Caballero, M.E.; Montero, M.P. Green Banana (*Musa Acuminata AAA*) Wastes to Develop an Edible Film for Food Applications. *Polymers* **2021**, *13*, 3183, doi:10.3390/polym13183183
32. Casado, S. Studying friction while playing the violin: Exploring the stick–slip phenomenon. *Beilstein J. Nanotechnol.* **2017**, 8, 159–166. https://doi.org/10.3762/bjnano.8.16
33. Casado, S.; Lobo, M.D.V.T.; Paino, C.L. Dynamics of plasma membrane surface related to the release of extracellular vesicles by mesenchymal stem cells in culture. Sci. Rep. 2017, 7, 6767. https://doi.org/10.1038/s41598-017-07265-x
34. Singh, N.; Singh, J.; Kaur, L.; Sodhi, N.S.; Gill, B.S. Morphological, thermal and rheological properties of starches from different botanical sources. *Food Chem*. **2003**, 81(2), 219-231. https://doi.org/10.1016/S0308-8146(02)00416-8
35. Quispe, M.; V. Lopez, O.; A. Villar, M. Oxidative Degradation of Thermoplastic Starch Induced by UV Radiation. *J. Renewable Mater.* **2019**, 7, 383–391. https://doi.org/10.32604/jrm.2019.04276
36. El-Hiti, G.A.; Ahmed, D.S.; Yousif, E.; Al-Khazrajy, O.S.A.; Abdallh, M.; Alanazi, S.A. Modifications of Polymers through the Addition of Ultraviolet Absorbers to Reduce the Aging Effect of Accelerated and Natural Irradiation. *Polymers* **2021**, 14, 20. https://doi.org/10.3390/polym14010020
37. Tarique, J.; Sapuan, S.M.; Khalina, A. Effect of Glycerol Plasticizer Loading on the Physical, Mechanical, Thermal, and Barrier Properties of Arrowroot (*Maranta Arundinacea*) Starch Biopolymers. *Sci. Rep.* **2021**, 11, 13900. https://doi.org/10.1038/s41598-021-93094-y
38. Taweechat, C.; Wongsooka, T.; Rawdkuen, S. Properties of Banana (*Cavendish Spp.*) Starch Film Incorporated with Banana Peel Extract and Its Application. *Molecules* **2021**, 26, 1406. https://doi.org/10.3390/molecules26051406
39. Dutta, D.; Sit, N. Comparison of Properties of Films Prepared from Potato Starch Modified by Annealing and Heat–Moisture Treatment. *Starch-Stärke* **2022**, 74, 2200110. https://doi.org/10.1002/star.202200110
40. Vamadevan, V.; Bertoft, E. Structure-function relationships of starch components. *Starch – Stärke* **2014**, 67, 1–2, 55–68. https://doi.org/10.1002/star.201400188
41. Domene-López, D.; García-Quesada, J.C.; Martin-Gullon, I.; Montalbán, M.G. Influence of Starch Composition and Molecular Weight on Physicochemical Properties of Biodegradable Films. *Polymers* **2019**, 11, 1084. https://doi.org/10.3390/polym11071084
42. Dai, L.; Zhang, J.; Cheng, F. Effects of Starches from Different Botanical Sources and Modification Methods on Physicochemical Properties of Starch-Based Edible Films. *Int. J. Biol. Macromol.* **2019**, 132, 897–905. https://doi.org/10.1016/j.ijbiomac.2019.03.197
43. Bergo, P.; Sobral, P.J.A.; Prison, J.M. Effect of glycerol on physical properties of cassava starch films. *J. Food Processing Preserv.* **2010**, *34*, 401–410.https://doi.org/10.1111/j.1745-4549.2008.00282.x
44. Pereira, J.F.; Garcia Lonni, A.A.S.; Mali, S. Development of biopolymeric films with addition of vitamin C and catuaba extract as natural antioxidants. *Prep. Biochem. Biotechnol.* **2022**, *52*, 1–10.https://doi.org/10.1080/10826068.2021.1916755
45. Wu, D.; Samanta, A.; Srivastava, R.K.; Hakkarainen, M. Starch-Derived Nanographene Oxide Paves the Way for Electrospinnable and Bioactive Starch Scaffolds for Bone Tissue Engineering. *Biomacromolecules* **2017**, *18*, 1582–1591. https://doi.org/10.1021/acs.biomac.7b00195
46. Pinto, J.; Dias, M.; Amaral, J.; Ivanov, M.; Paixão, J.A.; Coimbra, M.A.; Ferreira, P.; Pereira, E.; Gonçalves, I. *Influence of UV degradation of bioplastics on the amplification of mercury bioavailability in aquatic environments*. Marine Pollution Bulletin 2022, 180, 113806. https://doi.org/10.1016/j.marpolbul.2022.113806
47. Yin, P.; Zhang, Y.; Liu, X.; Wang, J.; Chen, L. *Surface cross-linked thermoplastic starch with different UV treatment effects studied by FTIR, mechanical and thermal analysis*. RSC Advances 2020, 10, 35677–35686.https://doi.org/10.1039/D0RA07549C

48. Bajer, D.; Kaczmarek, H.; Bajer, K. The Structure and Properties of Different Types of Starch Exposed to UV Radiation: A Comparative Study. *Carbohydr. Polym.* **2013**, 98, 477–482. https://doi.org/10.1016/j.carbpol.2013.05.090
49. Gutiérrez-Silva, K.; Capezza, A.J.; Gil-Castell, O.; Badia-Valiente, J.D. UV-C and UV-C/H_2O-Induced Abiotic Degradation of Films of Commercial PBAT/TPS Blends. *Polymers* **2025**, 17, 1173. https://doi.org/10.3390/polym17091173
50. Shahabi-Ghahfarrokhi, I.; Goudarzi, V.; Babaei-Ghazvini, A. Production of Starch Based Biopolymer by Green Photochemical Reaction at Different UV Region as a Food Packaging Material: Physicochemical Characterization. *Int. J. Biol. Macromol.* **2019**, 122, 201–209. https://doi.org/10.1016/j.ijbiomac.2018.10.154
51. Santacruz, S.; Rivadeneira, C.; Castro, M. Edible Films Based on Starch and Chitosan. Effect of Starch Source and Concentration, Plasticizer, Surfactant's Hydrophobic Tail and Mechanical Treatment. *Food Hydrocoll.* **2015**, 49, 89–94. https://doi.org/10.1016/j.foodhyd.2015.03.019
52. Pérez-Córdoba, L.J.; Galecio-Rojas, M.; Peña-Carrasco, F.; Ibarz, A.; Velezmoro-Sánchez, C.; Martínez-Tapia, P. *Effect of ultraviolet irradiation on physicochemical and disintegrability properties of tunta starch–tara gum nanocomposite films reinforced with starch nanocrystals*. Journal of Polymers and the Environment 2023, *31*, 299–311. https://doi.org/10.1080/25740881.2023.2285828.
53. Mahzan, S.; Fitri, M.; Zaleha, M. UV Radiation Effect towards Mechanical Properties of Natural Fibre Reinforced Composite Material: A Review. *IOP Conf. Ser.: Mater. Sci. Eng.* **2017**, 165, 012021. https://doi.org/10.1088/1757-899X/165/1/012021
54. Uyarcan, M.; Güngör, S.C. Improving Functional Properties of Starch-Based Films by Ultraviolet (UV-C) Technology: Characterization and Application on Minced Meat Packaging. *Int. J. Biol. Macromol.* **2024**, 282, 137085. https://doi.org/10.1016/j.ijbiomac.2024.137085
55. Velásquez-Castillo, L.E.; Leite, M.A.; Tisnado, V.J.A.; Ditchfield, C.; Sobral, P.J.D.A.; Moraes, I.C.F. Cassava Starch Films Containing Quinoa Starch Nanocrystals: Physical and Surface Properties. *Foods* **2023**, 12, 576. https://doi.org/10.3390/foods12030576